Modeling and Stochastic Control for Home Energy Management

Zhe Yu[†], Liyan Jia[†], Mary C. Murphy-Hoye[‡], Annabelle Pratt[‡], and Lang Tong[†]

***Abstract*—The problem of modeling and stochastic optimization for home energy management is considered. Several different types of load classes are discussed, including heating, ventilation, and air conditioning unit, plug-in hybrid electric vehicle, and deferrable loads such as washer and dryer. A first-order thermal dynamic model is extracted and validated using real measurements collected over an eight months time span. A mixed integer multi-time scale stochastic optimization is formulated for the scheduling of loads of different characteristics. A model predictive control based heuristic is proposed. Numerical simulations coupled with real data measurements are used for performance evaluation and comparison studies.**

***Index Terms*—Home energy management, model predictive control, demand response, temperature control, stochastic optimization.**

I. Introduction

THE idea of automated temperature control goes back over a hundred years when Warren Johnson invented a complete multi-zone temperature control system. The basic principle of temperature control has stood the test of time and can be applied to the general problem of home energy management (HEM) where energy is delivered to different types of load. The objective of HEM is to use energy efficiently for a comfortable and enjoyable living and working environment. Underlying this objective is the fundamental tradeoff between costs and quality of services.

The advent of "smart grid" will likely advance the state of the art of HEM in multiple dimensions. Some of the most important characteristics of HEM in a smart grid era include the extensive use of sensing devices, the optimal and automated management of different types of load, the integration of renewable energy and storage, and the ability to respond to dynamic prices.

In this paper, we consider scenarios in which a HEM device, serving as a control center, interfaces with the consumer and an electricity retail provider. Through the HEM device, the consumer participates in an economic demand response by managing energy consumption in response to dynamic pricing. The HEM device can also be used in an emergency demand response program where the retailer sets limits on power usage at times when the consumption needs to be curtailed.

[†]Z. Yu, L. Jia, and L. Tong are with the School of Electrical and Computer Engineering, Cornell University, Ithaca, NY 14853, USA. Email: {zy73, lj92, lt35}@cornell.edu. [‡]A. Pratt and M. Murphy-Hoye and are with the Intel Corp., USA.

This work is supported in part by the National Science Foundation under Grant CNS-1135844 and the Intel Corp.. Part of this work is presented at the 2011 CAMSAP in December 2011 and the IEEE PES General Meeting in July 2012.

A. Summary of results and contribution

The main contributions of this paper are in the modeling and optimization in HEM. On modeling, we present an empirical study aimed at extracting and validating a simple linear model based on the first law of thermal dynamics originally considered by Bargiotas and Birdwell [1]. In particular, we obtain model parameters using data collected over a period of eight months in Arizona and Oregon, two states with different weather conditions. The residential houses from which data are collected also have different heating and air conditioning equipments. While there is extensive literature on the thermal dynamic models of large facilities, there is limited result in the open literature on models for suburban residential homes using data of relatively large size. Our study shows that the linear time invariant state-space model holds well in one location in a 24 hours horizon whereas, in another location, the model holds well only in a two hours horizon. This suggests that, in general, a model used by a HEM system needs to be adaptive and model parameters need to be tracked, albeit at a relatively slower rate than the typical minute level sensing rate.

On optimization in HEM, we propose a stochastic and dynamic optimization framework with several features that, to our best knowledge, are new or have not been emphasized in existing approaches in the literature.

First, we formulate a constrained optimization where the consumer dissatisfaction measured by temperature deviation is minimized. The optimization is subject to maximum power, energy expenditure (monetary cost), and thermal dynamic constraints. The maximum power constraints are usually not considered in existing formulations. Making this constraint explicit allows the HEM device to respond not only to pricing signals but also to retailer imposed interruptions or load shedding requests. It can also be part of a hierarchical demand response system where an individual home receives power allocation as part of a community based demand response optimization [2]. The consumer expenditure constraint is also not part of most existing approaches. In our formulation, the HEM device optimizes consumer satisfaction given, for example, a monthly budget for energy consumption. This is a key to emancipating the consumer from real-time decisions on energy usage while removing the potential cost overrun at the end of a typical budget cycle.

Second, the proposed optimization framework operates in multiple time scales: sensing, control, and parameter estimation at a fast time scale (minutes), allocating energy expenditure to individual loads at a slow time scale (30 minutes to

an hour), satisfying cost constraints in even slower time scale (weeks or months). The partition of the energy management into slow and fast time scales significantly reduces computation complexity. To this end, we use the slow-time scale optimization to allocate energy expenditure to individual appliances. At the fast time scale, we perform separate optimization for each load class.

Third, because most existing heating, ventilation, and air conditioning (HVAC) units implement on-off controls, the underlying optimization involves integer decision variables. Finding the optimal on-off control sequence at the fast time scale does not have a computationally tractable solution. We show that, if the indoor-outdoor temperature difference does not vary significantly at the fast time scale, the problem of optimal on-off control can be approximated by the shortest path problem, which can be easily implemented by standard techniques.

B. Related work

The literature on home energy management is extensive and expanding. We focus here related work on the modeling and control aspects of HEM. Studies on thermal dynamic models for residential and commercial buildings date from 1978. The work reported in [3] used a convenient set of equivalent thermal parameters for residential townhouse. Our approach is based on the work of Bargiotas and Birdwell [1] who developed a simple linear dynamic model that involves a residential air conditioner. The power consumed by the air conditioner is the control input and outdoor temperature the exogenous random input. Our work in this paper focuses on the estimation and validation of this model for a modern HVAC system in a residential home.

There is a substantial literature on HEM control. In [4], the authors proposed the architecture of HEM system in the framework of spot price and formulated the control problem without maximum power constraints. Authors of [5] proposed a three-layer control mechanism and used Tabu search to find a feasible solution. In [6], particle swarm optimization was used to find the optimal solution for coordinately scheduling multiple energy resources. These approaches required accurate prediction of future energy usage. In [7], model and environmental uncertainties were incorporated into the proposed optimization framework. The developed control, however, was an open loop strategy without using real-time measurements.

The authors of [8] considered a similar scheduling problem as one treated in this paper. The emphasis in [8] was on the tradeoff between cost and waiting time in a multi-home setting. The work presented here focuses on energy management within a single home with a design tradeoff between cost and comfort level subject to budget and power constraints. It is also significant that the scheduling problem considered in this paper involves thermal dynamics that dictates the formulation of multi-stage stochastic dynamic optimization. The thermal dynamic was not modeled in [8] and the optimization involved was considerably simpler. The thermal dynamics were included in the HEM proposed for a single home in [9], using a direct search optimization. It was a single stage optimization which set the thermostat set points, whereas this work includes direct control of the HVAC system. In [10], thermal dynamic was included and a similar concept of multi-scale feedback control was proposed to manage the temperature and utilization of CPU. Utilization budget was calculated in slow time scale to maintain the temperature and in fast time scale CPU was distributed to tasks to meet the utilization set point.

The MPC strategy adopted in this paper goes back to [11], [12], and [13]. In [11], an algorithm referred to as LQG-MPC was proposed to deal with the state and control linear inequality constraints. In [12], and [13], the Quadratic Dynamic Matrix Control was used to solve nonlinear process optimization with state estimation. In [14], the flexible constraint handling capabilities of MPC were shown and the robust adjustments were surveyed in [15].

The current paper presents a hierarchical multi-timescale multi-stage approach to HEM. The two conference publications [16] and [17] that proceed the current paper include abbreviated description of the proposed approach and simulations. Additional new material that incorporates renewable energy source is also included in this journal version.

C. Organization and notations

This paper is organized as follows. Section II discusses the identification and validation of the thermal dynamic model based on real measurements collected in the states of Arizona and Oregon. Section III presents different characteristics of electricity loads and distributed renewable source in typical residential house and formulates the overall optimization problem as a quadratic stochastic programming. In section IV, we decompose the control problem into two time scales and propose a MPC based multi-stage multi-scale approach. Numerical results and comparison are presented in Section V.

Notions in this paper are standard. Because multiple timescales are involved, we use x_t for signal x in the slow timescale and $x[t]$ for the fast timescale counterpart. For convenience, variables are cataloged below.

NOMENCLATURE

$\hat{\alpha}_f, \hat{g}_f, \hat{c}_f$	Estimated fast time scale thermal parameters
α_f, g_f, c_f	Real fast time scale thermal parameters
A_f, G_f, C_f	Real fast time scale thermal parameter matrix
$\hat{A}, \hat{G}, \hat{C}$	Estimated slow time scale thermal parameter matrix
$\hat{A}_f, \hat{G}_f, \hat{C}_f$	Estimated fast time scale thermal parameter matrix
$\hat{x}[t+k\|t]$	State prediction given observation by time t
$\hat{x}^{\text{in}}[t]$	Predicted indoor temperature
$\Phi(*)$	Thermal dynamic equations
π	Scheduling policy
σ	Intensity of modeling noise
ε_m	Mean squared modeling error
ε_p	Mean squared prediction error
$\mathscr{Y}_{[0:t)}$	Information collected up to time t
B	Weekly or monthly budget
d_t	Slow time scale desired temperature

N_k Number of working minutes of HVAC planned at time t
$p^{\pi}[t]$ Total power consumption of policy π within time interval t.
$p^{\pi}_{\text{HVAC}}[t], p^{\pi}_{\text{PHEV}}[t], p^{\pi}_{\text{Def}}[t]$ Power consumption in interval t under policy π
$P^{\text{Def}}_{\text{rate}}$ Power rate of deferrable load
$p^{\text{HVAC}}[i]$ Fast time scale power allocation of HVAC
P^{HVAC}_t Continuous time power consumption of HVAC
$P^{\text{HVAC}}_{\text{max}}$ Maximum power limit of HVAC
$P^{\text{PHEV}}_{\text{max}}$ Maximum power limit of PHEV
p^{Renew}_t Slow time scale power output of renewable resource
P_t Total power limits within hour t
p^{Def}_t Slow time scale power expenditure of deferrable load
p^{HVAC}_t Slow time scale power expenditure of HVAC
p^{PHEV}_t Slow time scale power expenditure of PHEV
Q Desired charging amount of PHEV
s Starting time of deferrable load
T^{in}_t Continuous time indoor temperature
T^{out}_t Continuous time outdoor temperature
T_A, T_D Arrival and departure time of PHEV
T_d Predicted daily average outdoor temperature
T_E, T_L Earliest and latest starting time of deferrable load
T_f Number of stages in fast time scale optimization (*e.g.,* 60 minutes per hour)
T_s Number of stages in slow time scale optimization (*e.g.,* 24 hour per day)
T_w Number of stages in budget allocation (*e.g.,* 7 days per week)
$u[t] \in \{0, 1\}$ On-off status of HVAC
$v[t]$ Modeling noises vector
$v^{\text{in}}[t]$ Fast time scale indoor temperature modeling noise
v_t Slow time scale modeling noise
$w[t]$ Measurement noises vector
$x[t]$ Fast time scale state
$x^{\text{in}}_t, x^{\text{out}}_t$ Slow time scale state variables, indoor and outdoor temperature
$y[t]$ Fast time scale measurements
$y^{\text{in}}_t, y^{\text{out}}_t$ Slow time scale measurements
$z[t]$ Fast time scale electricity price
z_t Slow time scale electricity price
$\mathcal{C}(\pi)$ Economic cost under policy π
$\mathcal{D}(\pi)$ Temperature deviation under policy π
$\mathcal{R}$ $\mathcal{R} \triangleq \alpha_f(x^{\text{out}}[t] - x^{\text{in}}[t])$
$\mathcal{U}$ $\mathcal{U} \triangleq g_f P^{\text{HVAC}}_{\text{rate}}$

II. Model identification and validation

In this section, we present a first-order difference equation of the thermal dynamic model based on the work of Bargiotas and Birdwell [1]. Two data sets from Arizona and Oregon are described and different methodologies of model fitting are presented. The techniques used here are standard.

A. Thermal dynamic model

Thermal dynamic parameters vary from house to house, as well as human activity patterns. An electric heating-cooling thermal dynamic based upon the energy balance analysis presented in [1] is used in this paper. The first-order stochastic differential equation of the continuous temperature state T_t is stated as follows:

$$dT^{\text{in}}_t = a(T^{\text{out}}_t - T^{\text{in}}_t)dt + RP^{\text{HVAC}}_t dt + \sigma dv_t \tag{1}$$

where a is the thermal resistance related to the heat exchange between the outdoor and the indoor air, P^{HVAC}_t the power rate of the HVAC, and R the power efficiency. The temperature is driven by a Wiener process σdv_t with intensity σ. The Wiener process accounts for other heating/cooling sources such as human activities, refrigerators and dryers, etc.

The discrete-time equivalent equation for the continuous physical model is given by

$$\begin{aligned} x^{\text{in}}[t+1] = x^{\text{in}}[t] &+ \alpha_f(x^{\text{out}}[t] - x^{\text{in}}[t]) \\ &+ g_f p^{\text{HVAC}}[t] + c_f + v^{\text{in}}[t] \end{aligned} \tag{2}$$

where α_f, g_f, c_f are the essential thermal parameters to be estimated and $v^{\text{in}}[t]$ the system noise, assumed Gaussian and zero mean.

In a state space form with the possibility of including multiple HVAC units and multiple sensors, the matrix form of equation (2) is stated as:

$$\Phi(A_f, G_f, C_f) : \begin{cases} x[t+1] = A_f x[t] + G_f p^{\text{HVAC}}[t] \\ \qquad\qquad +C_f + v[t], \\ y[t] = x[t] + w[t]. \end{cases} \tag{3}$$

where $x[t]$ is the state vector, consisting of indoor temperatures in different rooms and the outdoor temperature. A_f reflects the heat exchange between rooms as well as the outdoor and the indoor air. G_f stands for the power efficiency of multiple HVAC units. $y[t]$ is the measurements of states. $v[t], w[t]$ are the modeling and measurement noise.

B. Data collection and measurements

Measurements were taken from one house in Arizona and one in Oregon. In the Arizona case, 3 HVAC units were used to cool 7 rooms. The data included outdoor temperature and insolation, HVAC power consumption and temperatures of different rooms. The data were collected every 15 minutes during August to November 2011 in Arizona. The Oregon data were collected similarly from January to April 2012. In this case, a two-stage furnace (high heat and low heat mode) was used to heat the room. The power consumption was computed from the cycle time of the furnace. As an example of typical measurement, Fig. 1 shows the indoor and outdoor temperatures, the power consumption, and the particular temperature set-point profile.

C. Model identification and validation

The parameters in model equation (2) can be obtained using the method of least squares:

$$\begin{aligned} (\hat{\alpha}_f, \hat{g}_f, \hat{c}_f) \quad = \quad & \underset{\alpha_f, g_f, c_f}{\operatorname{argmin}} \Big(\sum_{t=1}^{N} ||(x^{\text{in}}[t+1] - x^{\text{in}}[t]) \\ & -(c_f + \alpha_f(x^{\text{out}}[t] - x^{\text{in}}[t]) + g_f p^{\text{HVAC}}[t])||^2\Big) \end{aligned} \tag{4}$$

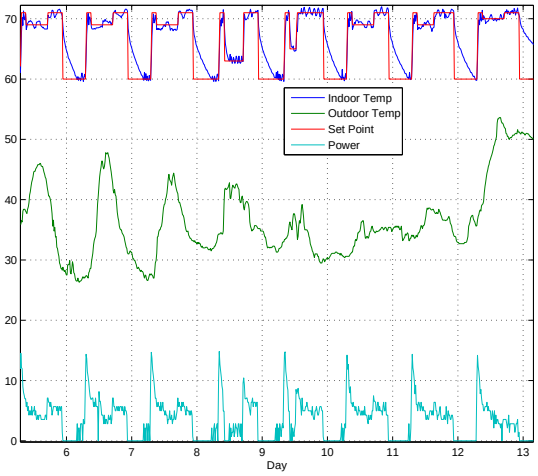

Fig. 1: Oregon data: Indoor Temp (°F), Outdoor Temp (°F), Set Point (°F), Power of furnace (kW/h)

where $N+1$ is the number of observations used in the parameter estimation. For time varying models, N should be large enough to obtain reliable estimates but small enough for the model remains stationary. In our study, we consider the cases where N corresponds to 1, 7, and 14 days of measurements.

The accuracy of the model can be measured by the mean squared *modeling error* (ME)

$$\varepsilon_m = \frac{1}{N}\sum_{t=1}^{N} ||(x^{\text{in}}[t+1]-x^{\text{in}}[t])-(\hat{c}_f+\hat{\alpha}_f(x^{\text{out}}[t]-x^{\text{in}}[t])+\hat{g}_f p^{\text{HVAC}}[t])||^2. \tag{5}$$

The model with estimated parameter using one set of data needs to be validated. To this end, we use a separate (un-used) data to test the predicability of the model. Specifically, given the estimated parameters $\hat{\alpha}_f, \hat{g}_f, \hat{c}_f$ obtained from one data set, we use a different set of data to test the accuracy of the one step prediction

$$\hat{x}^{\text{in}}[t+1] = x^{\text{in}}[t] + \hat{\alpha}_f(x^{\text{out}}[t] - x^{\text{in}}[t]) + \hat{g}_f p^{\text{HVAC}}[t] + \hat{c}_f, \tag{6}$$

The mean squared *prediction error* (PE) is given by

$$\varepsilon_p = \frac{1}{N}\sum_{t=1}^{N} ||\hat{x}^{\text{in}}[t+1] - x^{\text{in}}[t+1]||^2. \tag{7}$$

D. Results and observations

We describe in this section a summary of results and observations, leaving more detailed description in [18] and [19]. Given differences in weather conditions, heating and air conditioner equipments used in the residential houses, and consumer usage patterns, the techniques used for model identification were slightly different. The general observation was that the Arizona data appeared to support a more stationary model whereas the Oregon data suggested that the stationarity assumption seemed to hold for a relatively shorter time period and more adaptive modeling strategy seemed to be necessary.

We note that observations presented here are specific to the set of data used in this work.

1) The Arizona case: For the Arizona data collected during the month between August and November, we observe that a stationary within a one-day time horizon appeared to be adequate. Specifically, 96 measurement points (one point every 15 minutes) from previous day are used to extract one set of thermal parameters. Using this set of (α_f, g_f, c_f), the outdoor temperature measurement and the HVAC power, the indoor temperature of next day is forecasted.

A summary of Arizona data is shown in Table I. It is evident that, for most rooms, the modeling and prediction errors are quite small. One particular anomaly is the model fitting for the extra room which had a large prediction errors as well as a much greater standard deviation of indoor temperature. One explanation would be that there was another thermal source in this room which was not considered in the model. More extensive results can be found in [18].

TABLE I: Summary results of Arizona data

Room	$\overline{x_t^{\text{in}}}$(°F)	$\sigma_{x_t^{\text{in}}}$	ε_m	ε_p
Living Room	79.1244	1.8073	0.0103	0.0116
Family Room	80.5193	2.5919	0.0249	0.0282
Kitchen	81.8173	2.1409	0.0247	0.0281
Dining Room	79.0615	14.0744	0.1355	0.1480
Office Room	79.8312	9.6645	0.0879	0.0956
Hall	79.2099	1.1447	0.0182	0.0212
Extra Room	83.0398	48.2190	0.4122	29.8200
Ups. Office	78.2068	1.1281	0.0184	0.0199
Ups. bath	77.8422	2.6523	0.0372	0.0412

Thermal parameters of different rooms are summarized in Table II. Standard deviations of these estimates are relatively large which indicate that the model is not constant across time. The non-stationarity can be observed more clearly in Fig. 2. Thermal parameters, modeling errors and realization of real temperature and predictions of living room are plotted respectively. HVAC power efficient factor g varies with time while the modeling errors are small. An closer look at the real and predicted temperatures shows that the linear time invariant model follows the real temperature accurately.

TABLE II: Thermal Parameters of Arizona house

Room	$\bar{\alpha} \pm \sigma_\alpha$	$\bar{g} \pm \sigma_g$(°F/kWh)	$\bar{c} \pm \sigma_c$(°F)
Living Room	0.0083 ± 0.0046	-0.2076 ± 0.1211	0.0216 ± 0.0552
Family Room	0.0127 ± 0.0046	-0.1798 ± 0.1608	0.0062 ± 0.0908
Kitchen	0.0121 ± 0.0048	-0.1997 ± 0.1901	0.0324 ± 0.0894
Dining Room	0.0209 ± 0.0127	-0.5438 ± 0.1768	-0.0047 ± 0.1201
Office Room	0.0168 ± 0.0120	-0.5095 ± 0.2337	0.0176 ± 0.0802
Hall	0.0101 ± 0.0051	-0.3314 ± 0.1787	0.0264 ± 0.0669
Extra Room	0.0474 ± 0.0388	-5.8284 ± 24.6484	0.0709 ± 0.3141
Ups. Office	0.0107 ± 0.0048	-0.2990 ± 0.1214	0.0631 ± 0.0521
Ups. bath	0.0152 ± 0.0070	-0.4435 ± 0.6012	0.0417 ± 0.0820

By looking at the autocorrelation of modeling and prediction errors we analyze the relationship between errors and time. In

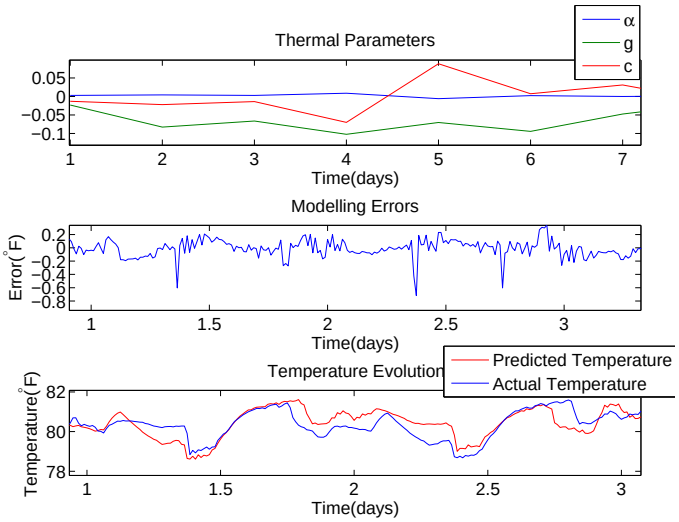

Fig. 2: Arizona data: Top: daily parameter estimates over time. Middle: modeling error example. Bottom: actual and predicted indoor temperatures.

Fig. 3 peaks can be found at every 96 lags indicating daily cycle in errors. A more comprehensive study of daily pattern may be needed.

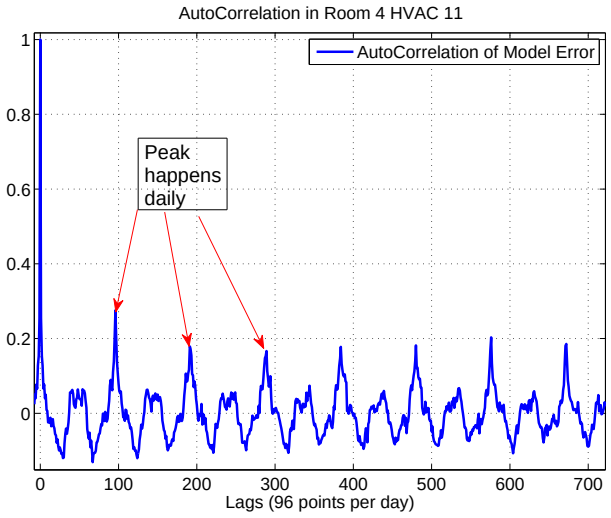

Fig. 3: Arizona data: Autocorrelation of modeling errors

Another important factor in model validation is the Gaussianity of the residue error. Although a rough analysis plotting cumulative distribution functions (CDF) of errors against the Gaussian CDF appears to endorse a close distribution, a careful examination using the Q-Q plot in Fig. 4 and Kolgomorov-Smirnov test indicates that the residues are non-Gaussian. Details can be found in [18].

2) The Oregon case: For the Oregon data, we can observe much significant non-stationarity, partly because of the specific

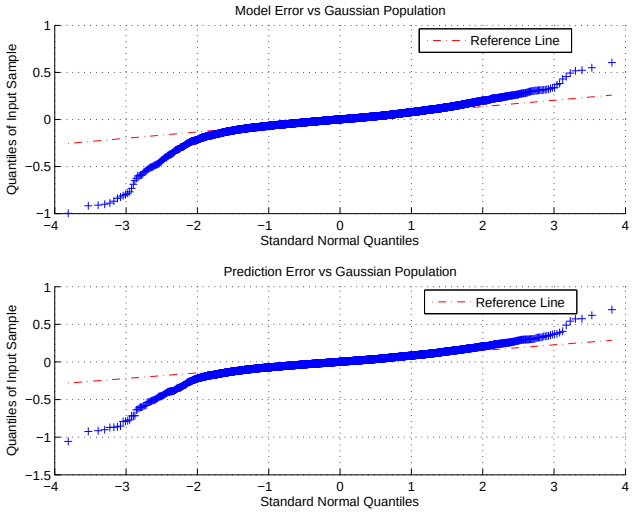

Fig. 4: Arizona data: Q-Q plot of modeling and prediction errors

heating system used by the resident. Table III summarizes the results of house in Oregon. One day fitting one day prediction methodology worked not well any more. The constant c, which stands for the un-modeled factor in the dynamic equation, is large. One possible reason is that a two-stage furnace unit was used in this house to heat and one constant thermal dynamic equation can not model it when the second coil was turned on to heat up the room rapidly. By looking at the residuals of one day fitting one day prediction shown in Fig. 5, we observe a daily pattern. The peaks around 7AM reflect the impact of human activities.

TABLE III: Results of Oregon house

	ε_p	$\bar{\alpha} \pm \sigma_\alpha$	$\bar{g} \pm \sigma_g$	$\bar{c} \pm \sigma_c$
One day fitting	0.6471	0.0933 ± 0.0597	0.1407 ± 0.0238	1.6986 ± 1.5965
Interval fitting	0.3625	0.0259 ± 0.0274	0.1267 ± 0.1116	0.3684 ± 0.5967

A more adaptive methodology is used for model identification. Specifically, measurements are divided into weekdays and weekends and each day is divided into 12 equal intervals. Measurements from the same intervals of previous 5 to 10 weekdays (weekends) are used for data training and estimating the thermal parameters. Thus total 12 models for different time periods are identified within a single day. The temperatures within the interval of the target day is predicted using the corresponding extracted parameters. For example, if the target period is 7AM to 9AM on Monday, measurements from 7AM to 9AM on last Monday to last Friday are used to extract one set of (α_f, g_f, c_f). We believe that this model captured the seasonal change as well as the human activities.

Temperature prediction and parameters realization of Oregon data are shown in Fig. 6. The prediction follows the actual temperature closely and there is a clear daily cycle in the thermal coefficients. Q-Q plots suggests non-Gaussianity as well. Details can be found in [19]

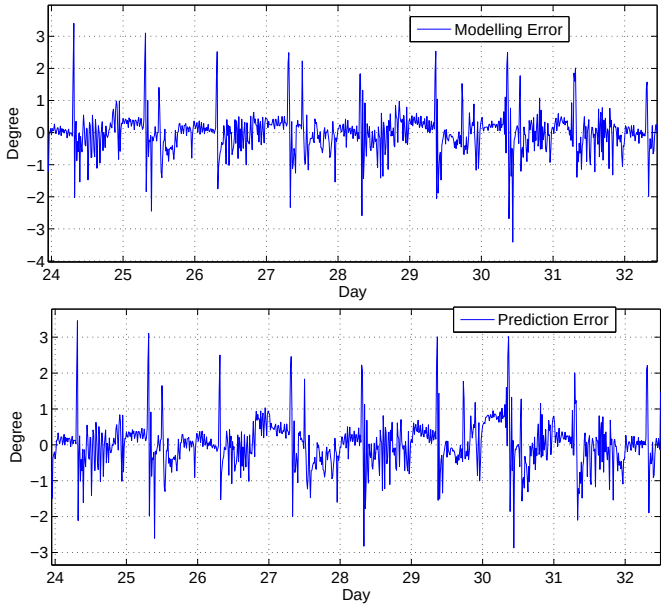

Fig. 5: Oregon data: modeling and prediction errors of one day fitting one day prediction method

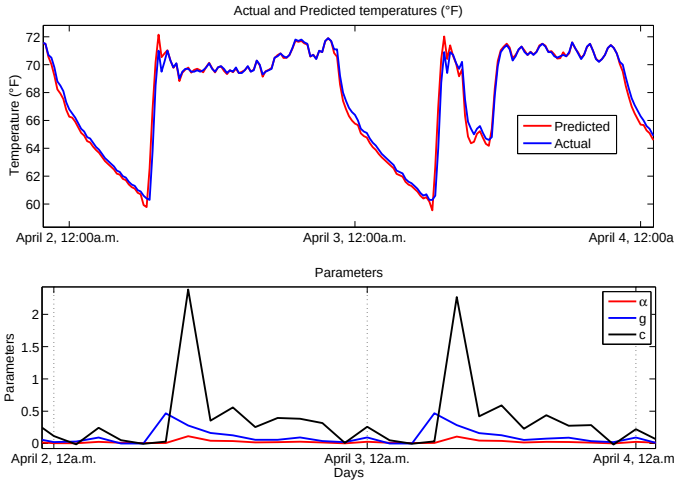

Fig. 6: Oregon data: Top: actual and predicted indoor temperature. Bottom: parameter estimates in a 2 hours interval

III. A HEM Optimization Framework

We describe in this section the proposed HEM architecture and related optimization with constraints. The specific techniques used in the optimization are described in Section IV.

A. Architecture of HEM

The HEM architecture considered in this paper is generic, illustrated in Fig 7. As a control center, the HEM device receives pricing information from the local utility or energy aggregator. In addition, the HEM device may also receive interruption or other control signals from the utility. In particular, we assume that the utility may limit the maximum power consumption during certain days or certain hours. Other information may also include local weather forecast.

The HEM device also interfaces with the consumer directly. It is assumed that the consumer input desired temperature profile that form the basis of measuring consumer satisfaction or quality of service. For certain appliances, the consumer specifies operation constraints. This may include, for example, the start time and deadline of plug-in hybrid electric vehicle (PHEV) charging or other deferrable load.

We focus here the interaction between the HEM device and the controllable appliances. This interaction is bi-directional; the HEM device takes sensor measurements and sends control signals to individual appliances.

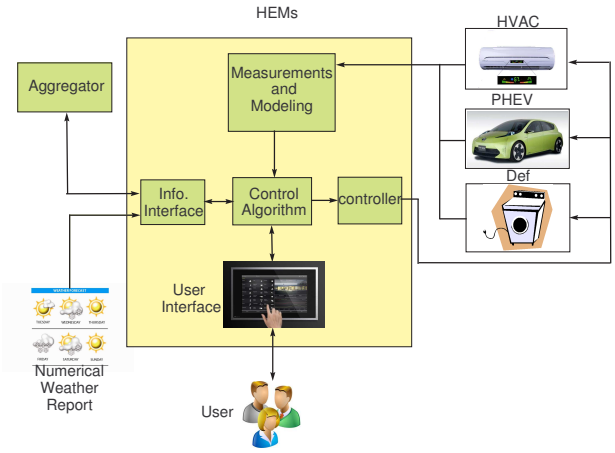

Fig. 7: Architecture of HEM

B. Load classes and assumptions

We consider three types of controllable demands: controllable dynamic load (HVAC), deferrable and interruptible load (PHEV charging), and deferrable and non-interruptible load (such as washer and dryer). We also consider the possibility of integrating local renewable resource (solar panel)

The model of dynamic load (HVAC) has been discussed earlier in Section II. Implicitly assumed here is that the model used in the optimization is tracked or updated periodically. We assume that the HVAC is subjected to on-off control only.

We consider PHEV charging as a deferrable and interruptible load. In particular, charging can be temporarily suspended and resumed at a different time. The charging time and amount within each period are part of the optimization. The arrival and departure time of PHEV are assumed specified and a desired amount of charging should be delivered by the deadline. Specifically, the charging deadline is a hard constraint with a higher priority than temperature comfort. Similar approach can be found in [9]. The work presented in [20] discussed a strategy that took into account battery degradation, which we ignore here.

The deferrable and non-interruptible loads have the flexibility of optimizing starting time. Once a task starts, it has to be completed. We assume that we are given the hard constraints on the earliest and latest starting time. We assume in the simulation that the deferrable and non-interruptible load draws constant rated power $P^{\text{Def}}_{\text{rate}}$.

Distributed renewable energy is considered as an additional power resource of the house. The solar panel is considered as an example in this paper. During the day time, solar panel could provide power to the house which helps to alleviate the energy and budget shortage. The output of the solar panel is assumed not controllable but predictable with noises and not enough to cover all the power usage in this paper.

C. Control policy, performance measure, and constraints

Optimization is used to derive a *control/scheduling policy* π that maps the information $\mathscr{Y}_{[0:t)}$ collected via interface and the measurements up to time t to the power allocation to the loads $(p^{\pi}_{\text{HVAC}}[t], p^{\pi}_{\text{PHEV}}[t], p^{\pi}_{\text{Def}}[t])$ at the fast time scale (at intervals of one or several minutes).

The performance of the control policy π is measured by consumer satisfaction. In this paper, since we impose a budget constraints on energy expenditure and require that all deferrable loads are served before deadlines, the consumer satisfaction is measured only by the temperature deviation from the desired set points, *i.e.*,

$$\mathcal{D}(\pi) \triangleq \mathbb{E}_{\pi}\Big(\sum_{t} \|x^{\text{in}}[t] - d[t]\|^2\Big). \tag{8}$$

We assume that the consumer is a price taker. Given the price of electricity $z[t]$, the cost of control policy π is given by

$$\mathcal{C}(\pi) \triangleq \sum_{t} z[t] \times p^{\pi}[t], \tag{9}$$

where $p^{\pi}[t] = p^{\pi}_{\text{HVAC}}[t] + p^{\pi}_{\text{PHEV}}[t] + p^{\pi}_{\text{Def}}[t]$ is the total power consumption within time interval t.

In addition to the thermal dynamic constraint, we impose the following types of constraints:

1) *Budget (cost) constraint:* We assume that the consumer specifies a long term budget constraint B in the form of weekly or monthly dollar amount. In our approach, B is broken into daily budget B_d which is adaptively adjusted from one day to the other. See Section IV-C for a budget allocation scheme.
2) *Maximum power constraint:* We assume that there is a maximum power consumption limit imposed either by the utility or an energy aggregator. Such a constraint may be mandated as part of certain demand response program for which the consumer may receive lowered rate for accepting such limits.
3) *Scheduling constraints:* We assume that deferrable loads are specified by their deadlines. Assuming feasibility, such scheduling constraints are always met.

We now have the detailed constrained optimization as follows

$$\begin{aligned}
\text{minimize} \quad & \textstyle\sum_{t=1}^{T_s \times T_f} \mathbb{E}_{\pi}\|x^{\text{in}}[t] - d[t]\|^2 \\
\text{subject to} \quad & 1.\ (x[t], y[t]) \sim \Phi(A_f, G_f, C_f) \\
& 2.\ p^{\text{HVAC}}[t] \in \{P^{\text{HVAC}}_{\max}, 0\} \\
& 3.\ T_E \le s \le T_L \\
& 4.\ p^{\text{Def}}[t] = \begin{cases} P^{\text{Def}}_{\text{rate}} & \text{if } s \le t < s+d \\ 0 & \text{o.w.} \end{cases} \\
& 5.\ 0 \le p^{\text{PHEV}}[t] \le P^{\text{PHEV}}_{\max} \\
& 6.\ \textstyle\sum_{t=1}^{T_s \times T_f} p^{\text{PHEV}}[t] = Q \\
& 7.\ p^{\text{PHEV}}[t] = 0 \quad \text{if } t < T_A \text{ or } t > T_D \\
& 8.\ \textstyle\sum_{t=T_f \times (i-1)+1}^{T_f \times i} (p^{\text{HVAC}}[t] + p^{\text{PHEV}}[t] \\
& \qquad + p^{\text{Def}}[t] - p^{\text{Renew}}[t]) \le P_i \quad i = 1, \ldots, T_s \\
& 9.\ \textstyle\sum_{t=1}^{T_s \times T_f} z[t](p^{\text{HVAC}}[t] + p^{\text{PHEV}}[t] + p^{\text{Def}}[t] - p^{\text{Renew}}[t]) \le B_d
\end{aligned} \tag{10}$$

where the indoor temperature vector $x^{\text{in}}[t]$ is part of the state evolution $(x[t], y[t]) \sim \Phi(A_f, G_f, C_f)$ specified by the stochastic thermal dynamic equation (3). The control variables $(p^{\text{HVAC}}[t], p^{\text{PHEV}}[t], s)$ in this optimization are fast time-scale power allocation for HVAC, PHEV and the starting time of deferrable and non-interruptible load. Note that once s is determined, the power consumption $p^{\text{Def}}[t]$ is fixed.

The global objective is to minimize the expected temperature deviation over a whole day, where the state follows the thermal dynamic model in constraint (1) and the control of HVAC is an On-off control as stated in constraint (2). Constraints (3-4) describe the deferrable and non-interruptible load, which has to start between T_E and T_L, and work consistently for time d. Constraints of PHEV are stated as (5-7). $p^{\text{PHEV}}[t]$ is assumed to be continuous and a desired amount of charging, Q, is required to be delivered between T_A and T_D. The total power consumption within ith hour should not exceed the power limit P_i and the total cost is bounded by daily budget B_d

The above optimization is a mixed integer program with a high dimensional state space. The main challenge of this optimization comes from the power limit and budget constraints in (8-9) which bundle all control variables. In the next section, we present a multi-scale model predictive control approach that unbundles these variables.

IV. Multi-scale Model Predictive Control

In this section, we present the multi-scale control architecture of HEM system shown in Fig. 8 based on the principle of model predictive control. The proposed optimization problem (10) is decomposed into two time-scales. The HEM system distributes the hourly power expenditure to different devices at the slow time scale. In the fast time scale, HEM system measures the temperatures, extracts thermal parameters and predicts the thermal dynamic state $\hat{x}[t+k|t]$ into the future using Kalman filter. Since loads are decoupled in the slow time scale, HEM system can optimize the detailed power allocation of loads individually at the fast time scale. In both time scales, only first step is implemented and HEM system resolves the problem again with latest observations.

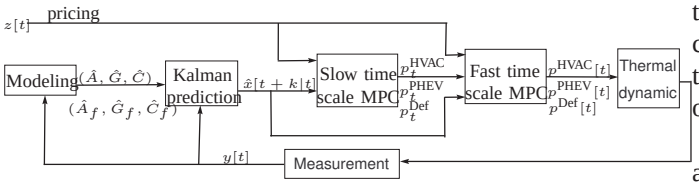

Fig. 8: Multi-scale HEM architecture

The MPC based suboptimal approach to the HEM stochastic problem is detailed described in Table IV. The slow and fast scale problems are discussed individually in this section.

A. Slow time scale stochastic optimization

We decompose the overall optimization (10) into two time-scales. In the slow time scale, HEM system distributes power expenditure to different loads and decouple them from the power limits and the budget constraints. The slow time scale problem is formulated as follows:

$$\begin{array}{ll}
\text{minimize} & \sum_{i=1}^{T_s} \mathbb{E}\|x_i^{\text{in}} - d_i\|^2 \\
\text{subject to} & (x_i, y_i) \sim \Phi(\hat{A}, \hat{G}, \hat{C}) \\
& 0 \le p_i^{\text{HVAC}} \le P_{\text{max}}^{\text{HVAC}} \\
& \\
& T_E \le s \le T_L \\
& p_t^{\text{Def}} = \begin{cases} P_{\text{rate}}^{\text{Def}} & \text{if } s \le t < s+d \\ 0 & \text{o.w.} \end{cases} \\
& 0 \le p_i^{\text{PHEV}} \le P_{\text{max}}^{\text{PHEV}} \\
& \sum_{i=1}^{T_s} p_i^{\text{PHEV}} = Q \\
& p_i^{\text{PHEV}} = 0 \quad \text{if } i < T_A \text{ or } i > T_D \\
& \\
& 0 \le p_i^{\text{HVAC}} + p_i^{\text{PHEV}} + p_i^{\text{Def}} \le P_i + p_i^{\text{Renew}}, i = 1, \cdots, T_s \\
& \sum_{i=1}^{T_s} z_i (p_i^{\text{HVAC}} + p_i^{\text{PHEV}} + p_i^{\text{Def}} - p_i^{\text{Renew}}) \le B_d
\end{array} \tag{11}$$

Different from the formulation of the overall problem (10), HEM system only optimizes power expenditure at slow time scale and p_i^{HVAC} is a continuous variable.

To deal with home appliances which are starting in the middle of a slow time scale interval, HEM system needs to scale the maximum power constraints of these loads proportional to the fraction of available working time within that interval. For example, the PHEV arrives home at 7:40 and the maximum charging rate within that hour will be set as $\frac{1}{3}P_{\text{max}}^{\text{PHEV}}$. For simplicity, we assume all the loads start in the beginning of the intervals in this paper.

B. Fast time scale stochastic optimization

Receiving the slow time scale power expenditure as constraints, HEM system schedules loads in the fast time scale to meet the requirements and minimize the temperature deviation. In the fast time scale problem, the MPC principle applies as well, except that for HVAC and some loads we are dealing with integer control variables.

The control problems of various devices are decomposed in the slow time scale problem so we can consider them individually. The starting time of deferrable and non-interruptible determines the power allocation trivially. If we can assume the charging rate of PHEV is continuous, the fast time scale charging problem is just a linear programming. In this paper, the electricity price is assumed constant over one hour, so we omit the fast time scale problem for dryer and PHEV.

When focussing on the control problem of HVAC, we are dealing with a integer programming. The fast time scale problem of HVAC is formulated as follows:

$$\begin{array}{ll}
\min_{u[i]} & \sum_{i=1}^{T_f} \mathbb{E}\|x^{\text{in}}[i] - d[i]\|^2 \\
\text{subject to} & (x[i], y[i]) \sim \Phi(\hat{A}_f, \hat{G}_f, \hat{C}_f) \\
& p^{\text{HVAC}}[i] = u[i] P_{\text{rate}}^{\text{HVAC}} \\
& u[i] \in \{0, 1\} \\
& \sum_{i=1}^{T_f} u[i] \le \frac{p_k^{\text{HVAC}}}{P_{\text{rate}}^{\text{HVAC}}}
\end{array}$$

where p_k^{HVAC} is the power budget assigned by the HEM device at the slow time scale.

The most widely used HVAC control strategy is the rule based control (RBC) or bang bang control. It is a control restricted between a lower and an upper bound around the set points [21]. In practice, the length of the interval between HVAC on-off states switching may be an additional constraint as it influences the longevity. A benchmark solution of the fast time scale problem is to relax the $0-1$ constraint $u[i] \in \{0, 1\}$ by a continuous one $u[i] \in [0, 1]$. The relaxed problem gives us an lower bound of the performance. Similar relaxation problem is discussed in [22].

Within the class of integer optimization, we formulate the problem as that given the slow time scale power expenditure, we choose the working periods of HVAC to minimize the deviation of indoor temperature from the set points. Once the switching time is determined, the HEM can implement the control of HVAC by artificially changing the set point without actually installing an extra device.

Given the hourly power expenditure p_k^{HVAC}, we calculate the number of working periods (minutes) of HVAC by $N_k = \lceil p_k^{\text{HVAC}} / P_{\text{rate}}^{\text{HVAC}} \rceil$. The allocation of the working periods is formulated as a stochastic programming with a binary action space, which is still computationally intractable. But we can approximate this as an shortest path problem by assuming the changes of indoor and outdoor temperature are small within one hour. At time t, we approximate the future outdoor indoor temperature gap, $(x^{\text{out}}[t+i] - x^{\text{in}}[t+i])$, as the initial one, $(x^{\text{out}}[t] - x^{\text{in}}[t])$.

At the tth minute, denote the initial temperature difference as $\mathcal{R} \triangleq \alpha_f (x^{\text{out}}[t] - x^{\text{in}}[t])$ and the HVAC power effect as $\mathcal{U} \triangleq g_f P_{\text{rate}}^{\text{HVAC}}$. The future temperature at $(t+i+1)$th minute is approximated as:

$$\begin{array}{rcl}
x^{\text{out}}[t+i+1] & \approx & x^{\text{out}}[t] \\
x^{\text{in}}[t+i+1] & = & x^{\text{in}}[t+i] + \alpha_f (x^{\text{out}}[t+i] - x^{\text{in}}[t+i]) \\
& & + g_f P_{\text{rate}}^{\text{HVAC}} u[t+i] \\
& \approx & x^{\text{in}}[t+i] + \alpha_f (x^{\text{out}}[t] - x^{\text{in}}[t]) \\
& & + g_f P_{\text{rate}}^{\text{HVAC}} u[t+i] \\
& \approx & x^{\text{in}}[t] + (i+1) \times \mathcal{R} \\
& & + \mathcal{U} \sum_{k=0}^{i} u[t+k]
\end{array}$$

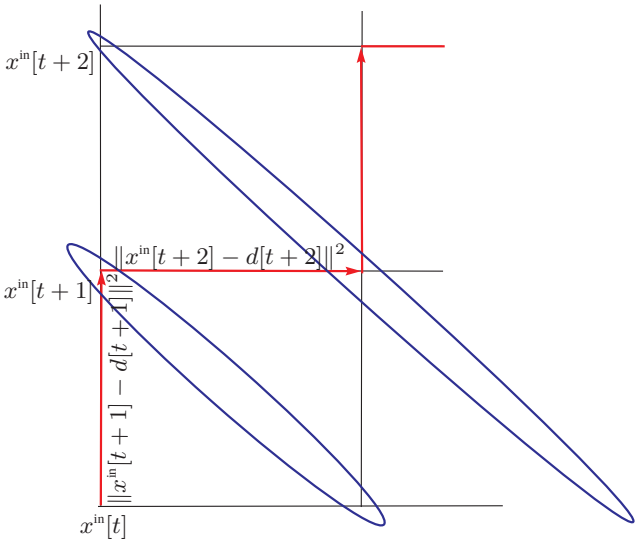

Fig. 9: Shortest path formulation

The approximation problem can be formulated as follows: at minute t, solve the dynamic programming problem:

$$\begin{array}{ll}\min_{\hat{u}[i]} & \sum_{i=t+1}^{T_f}\|x^{\text{in}}[i]-d[i]\|^2\\ \text{subject to} & x^{\text{in}}[t+i]=x^{\text{in}}[t]+i\times\mathcal{R}+\mathcal{U}\sum_{k=0}^{i-1}\hat{u}[t+k]\\ & \sum_{i=t}^{T_f}\hat{u}[i]=N_k-\sum_{j=1}^{t-1}u[j]\\ & \hat{u}[i]\in\{0,1\}\end{array}$$

Consider a grid as shown in Fig. 9. At time t, the vertices are defined as the future indoor temperatures at time $t, t+1, \ldots, T_f$ under different strategy scenarios and the distance between adjacent vertices is defined as the temperature deviation of the $(t+i+1)$th minute, $(\|x^{\text{in}}[t+i+1]-d[t+i+1]\|^2)$. Going upward means the HVAC will be working for the next minute (u[t+i]=1) while going right means not (u[t+i]=0). So we have a single-source (left bottom of the grid) single-destination (right top of the grid) shortest path problem with a grid size of $(N_k-\sum_{j=1}^{t-1}u[j])\times[T_f-t-(N_k-\sum_{j=1}^{t-1}u[j])]$. This problem can be well solved by Dijkstra's algorithm. Considering the approximation may not be accurate, we apply the MPC principle here. At the beginning of every minute we solve the shortest path problem and apply the first $u[i]$ and at the beginning of the next minute we solve the updated problem again.

It is true that the power consumed in the fast time scale stage may be less than the power expenditure allocated in the slow time scale stage, *i.e.*, $p_{\text{rate}}^{\text{HVAC}}\sum_{i=1}^{T_f}u[i]\le p_k^{\text{HVAC}}$. We just put the residual back to the budget pool and reuse it in the future.

C. Budget Allocation

At the beginning of a week or a month, HEM device receives the total budget setting from the users and distributes the money into everyday according to the weather information from numerical weather report and the activity information

TABLE IV: Model Predictive Control in Slow and Fast Time Scales

Model Predictive Control in Slow Time Scale

1 At hour t, compute Kalman state predictions $\hat{x}_{t+k|t}$ using y_t.
2 Obtain the optimal starting time s^* by minimizing the cost of deferrable load.
3 Solve for $(\hat{p}_i^{\text{HVAC}},\hat{p}_i^{\text{PHEV}})_{i=t}^{T_s}$ by the quadratic optimization:

$$\begin{array}{ll}\text{minimize} & \sum_{i=t+1}^{T_s}\left(\|x_{i|t}^{\text{in}}-d_i\|^2\right)\\ \text{subject to} & (x_i,y_i)\sim\Phi(\hat{A},\hat{G},\hat{C})\\ & 0\le\hat{p}_i^{\text{HVAC}}\le P_{\text{max}}^{\text{HVAC}}\\ & 0\le\hat{p}_i^{\text{PHEV}}\le P_{\text{max}}^{\text{PHEV}}\\ & \sum_{i=t}^{T_s}\hat{p}_i^{\text{PHEV}}=(Q-\sum_{k=1}^{t-1}Tp_k^{\text{PHEV}})^+\\ & \hat{p}_i^{\text{PHEV}}=0\quad\text{if } i<T_A \text{ or } i>T_D\\ & 0\le\hat{p}_i^{\text{HVAC}}+\hat{p}_i^{\text{PHEV}}+\hat{p}_i^{\text{Def}}\le P_i+\hat{p}_i^{\text{Renew}},\ i=t,\cdots,T_s\\ & \sum_{i=t}^{T_s}z_i(\hat{p}_i^{\text{HVAC}}+\hat{p}_i^{\text{PHEV}}+\hat{p}_i^{\text{Def}}-\hat{p}_i^{\text{Renew}})\\ & \quad\le\left(B_d-\sum_{k=1}^{t-1}z_k(p_k^{\text{HVAC}}+p_k^{\text{PHEV}}+p_k^{\text{Def}}-p_k^{\text{Renew}})\right)^+\end{array}$$

4 Set $p_t^{\text{HVAC}}=\hat{p}_t^{\text{HVAC}}$ and $p_t^{\text{PHEV}}=\hat{p}_t^{\text{PHEV}}$.
5 $t\to t+1$, go to line 1 until $t=T_s$

Model Predictive Control in Fast Time Scale

1 At minute t, compute Kalman state predictions $\hat{x}^{\text{in}}[t+k|t]$ using y_t.
2 Solve for $\hat{u}[i]$ by the quadratic optimization:

$$\begin{array}{ll}\text{minimize}_{\{\hat{u}[i]\}} & \sum_{i=t+1}^{T_f}\|x^{\text{in}}[i|t]-d[i]\|^2\\ \text{subject to} & (x[i],y[i])\sim\Phi(\hat{A}_f,\hat{G}_f,\hat{C}_f)\\ & p^{\text{HVAC}}[i]=\hat{u}[i]P_{\text{rate}}^{\text{HVAC}},\quad\hat{u}[i]\in\{0,1\}\\ & \sum_{i=t}^{T_f}\hat{u}[i]=N_k-\sum_{j=1}^{t-1}u[j].\end{array}$$

3 Set $u[t]=\hat{u}[t]$.
4 $t\to t+1$, go to 1 until $t=T_f$

from calendar. Assuming HEM device is cooling the house, one direct way is to distribute the budget in proportion to the forecasted daily average outdoor temperature. Another one is known as water filling in communication. Similarly, the money is distributed to every particular day according to the predicted outdoor temperature by solving the following optimization problem:

$$\begin{array}{ll}\text{maximize} & \sum_{d=t}^{T_w}\log(1+\frac{B_d}{T_d})\\ \text{subject to} & \sum_{d=t}^{T_w}B_d=B\end{array}\qquad(12)$$

where B is the total budget, B_d is the daily budget and T_d is the predicted daily average outdoor temperature. The optimal solution can be viewed as filling the daily temperature curve by the budget as shown in Fig. 10

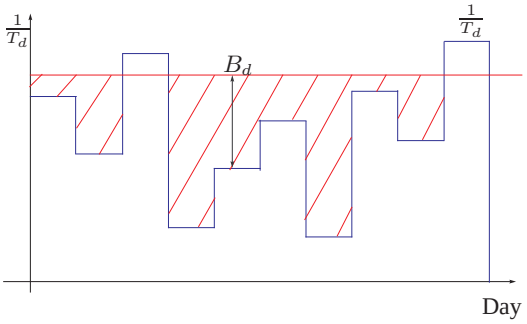

Fig. 10: Water filling budget allocation

Considering that the long term weather report is not reliable, we employ the rolling scheme here. At the end of every hour,

if the budget is not used up, HEM device will put it back to the rest of total budget pool and allocate the daily budget again with updated information.

V. Simulation and Performance Results

In this section, an scheduling example is shown at the beginning, followed by the comparison between proposed MPC algorithm with the RBC and other benchmarks based on real measurements. In the end, the shortest path performance is discussed.

First of all, scheduling of three different kinds of loads without renewable energy is considered in the simulation. A PHEV is assumed available from 8PM to 8AM. The charging rate is nonnegative which implies it can not supply energy back to the grid. The washer/dryer, as an example of deferrable and non-interruptible load, is assumed to work for 2 hours, starting no earlier than 4PM and no later than 8PM. The power rate is assumed constant. The power limits profile, simply assumed to be a sinusoid curve, and the daily budget are constraints given to HEM.

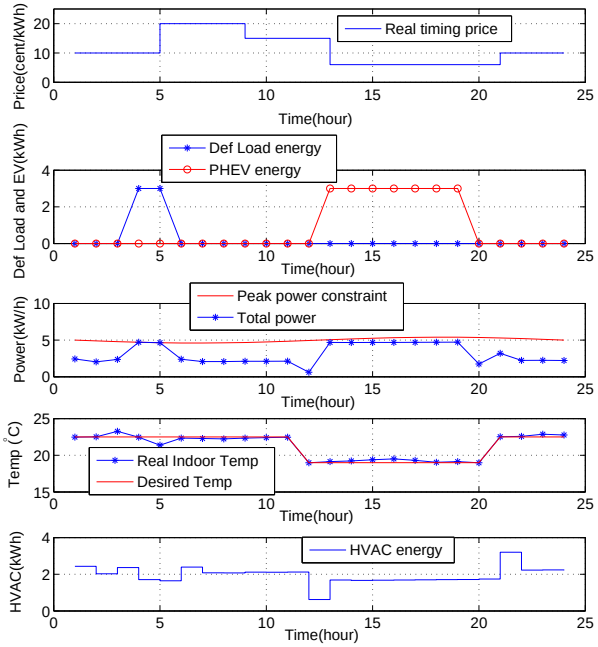

Fig. 11: Power policy example: price, dryer and PHEV charing, total power and peak power constraints, indoor temp, HVAC

The power policy example is illustrated in Fig. 11. Recall that the global objective is to minimize the temperature deviation. The scheduling of PHEV and washer/dryer affects the temperature deviation indirectly through the peak limit constraints and economic budget constraints. In Fig. 11, to yield budget to HVAC, the charging of PHEV is shifted to the price valley. The washer/dryer takes a relatively lower price period because of the tighter deadline. Note that the peak power constraint is bounded in some periods and the power allocated to HVAC, with a lower priority, is limited. So the indoor temperature deviates from the set points.

To show the performance of proposed MPC approach, it is compared with some benchmark solution using extracted thermal parameters and weather information. Note that the deferrable loads do not appear in the objective function and affect the discomfort level only via peak power constraints and total economic budget. The control of HVAC is simulated and other loads are removed from these two constraints.

In the simulation, the benchmarks include rule based control (RBC), performance bound (PB) and an algorithm combining the MPC and the LQG (thus referred to as MPC-LQG) originally proposed in [11]. When the constraints are loose, MPC-LQG performs closely to LQG, which is the optimal solution to the unconstrained stochastic programming problem. When the constraints are tight, the performance of MPC-LQG is close to open loop control. The performance bound is obtained by assuming the system noise and weather condition in the future are perfectly known.

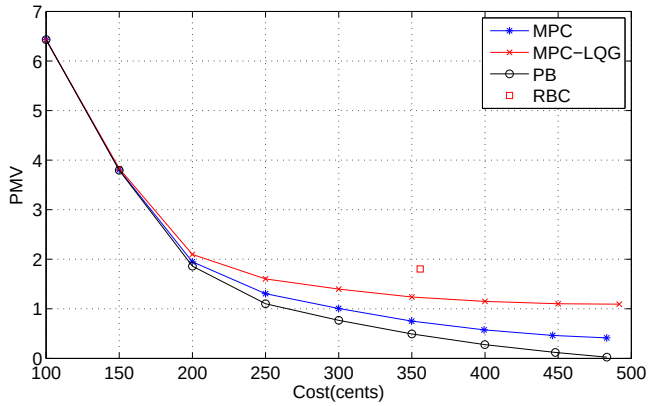

Fig. 12: 1 day performance comparison between multi-scale algorithm (MPC), MPC-LQG, PB and RBC

Assuming the outdoor temperature follows an auto-regression model, the performances of algorithms are shown in Fig. 12. The discomfort level, which is measured based on Predicted Mean Vote (PMV) [23], against total energy cost is plotted. In this paper, the tolerance region is set zero and the absolute value of temperature deviation from set points are used as PMV. In Fig. 12, at the same discomfort level, the proposed approach saves around 20% comparing to MPC-LQG and spends about 8% more than the performance bound. Comparing to RBC, the multi-scale approach maintains the same comfort level with 30% less cost. The performance of different algorithm appears the same when there is a tight budget constraint, which is because all strategies have limited power to allocate.

To show the impact of model accuracy on performance of MPC, the comparison between different outdoor temperature prediction noise is drawn in Fig. 13. With the same power and budget constraints, the discomfort level of MPC reduces fast with the decreasing of the noise. The performance of RBC does not change because RBC does not rely on the forecasting. When the prediction is accuracy, the gap between MPC and

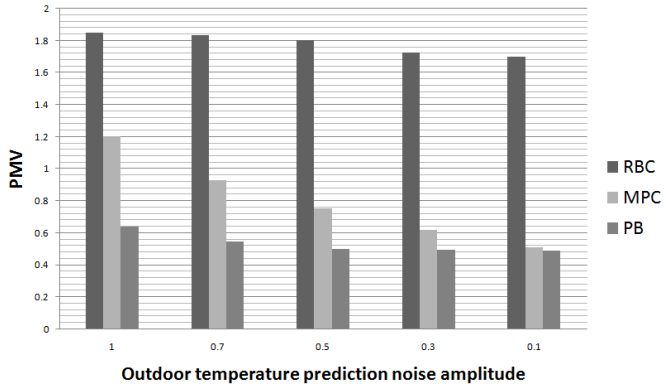

Fig. 13: Performance comparison between RBC, PB and multi-scale algorithm (MPC) with various outdoor temperature noises

performance bound is negligible.

We compare the performance of the multi scale algorithm with the real RBC control of HVAC based on the real measurement data from Arizona, in Fig. 14. The discomfort level of RBC is calculated from the indoor temperature measurements and the power consumption is from the power meter. In the simulation, MPC uses data from pervious day to build the thermal model and uses the parameters to predict and allocate power to HVAC for the next day. While the indoor temperature changes following the dynamic equation with the real thermal parameters of the target day. To show the impact of the accuracy of the thermal model, the same MPC algorithm assuming knowing real parameters is plotted as a comparison. At the same discomfort level of RBC, the multi-scale algorithm saves about 12% and the gap between MPC and PB is less than 2%.

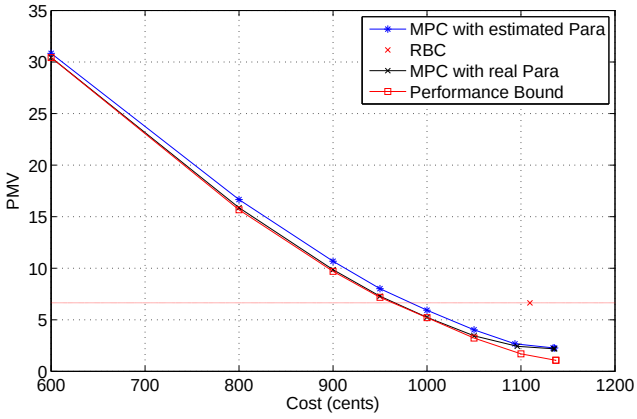

Fig. 14: Arizona data: 10 days performance comparison between RBC, PB and multi-scale algorithm (MPC)

A similar simulation, which heating the house instead of cooling, is carried out based on the measurements from Oregon shown in Fig. 15. The performance of RBC is also simulated. By relaxing the lower bound, we plot the performance curve of RBC as well as the actual performance calculated from measurements. The simulated RBC differs from the measurements because of the modeling errors. At the same comfort level, multi-stage algorithm saves more than 30% comparing to the performance of RBC calculated using real measurements.

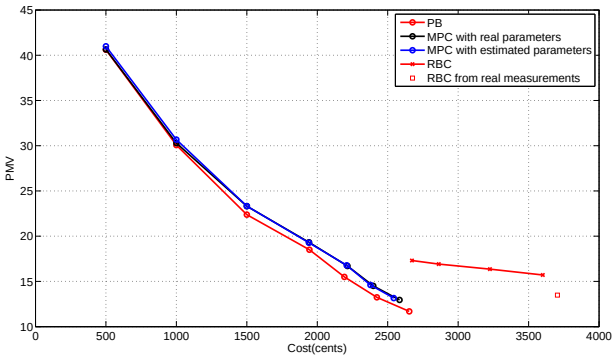

Fig. 15: Oregon data: 5 days performance comparison between RBC , PB and multi-scale algorithm (MPC)

To see the impact of renewable energy, we include the solar panel in the optimization as an alternative power resource. In Fig. 16, the output of the solar panel is assumed predictable with noise. Since the solar power not only alleviates the peak power limits but also the budget, the discomfort level is lower with cheaper energy cost. At the same discomfort level, MPC algorithm saves more than 50% comparing to RBC from measurements. While without solar power, the saving is around 22%.

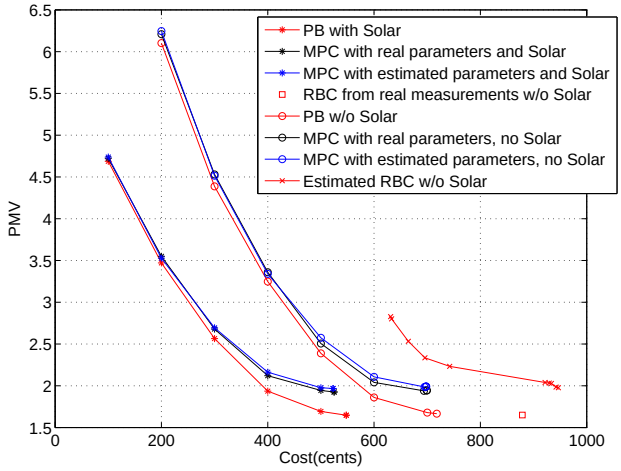

Fig. 16: Oregon data: 1 days performance comparison between RBC, PB and multi-scale glgorithm (MPC) associated with solar power

To show the efficiency of shortest path algorithm in fast time scale optimization we compare the shortest path approach

with the optimal solution to the relaxed continuous problem. In Fig. 17, simulation is carried out based on the extracted thermal parameters. At the same comfort level, the gap is less than 5%, which implies the performance of the shortest path is a reasonable approach to approximate the original problem.

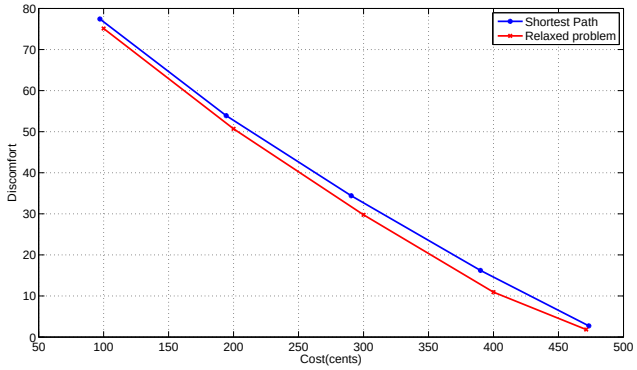

Fig. 17: Shortest path approach vs relaxed solution

VI. Conclusion

A Home energy management (HEM) system, as a key component of demand response in smart grid, should be able to control various residential loads based on the user requirement and other information. We formulate the control problem of HEM in this paper as a multi-stage stochastic programming problem. The HEM system acts as an interface between users and aggregators to exchange the real-time pricing signal and power consumption limits. Using the measurements and numerical weather report, the HEM system optimizes the power allocation to minimize the user discomfort level. A multi-scale computationally tractable suboptimal approach is proposed to solve the stochastic programming problem. First order thermal dynamic model is validated and online thermal parameter estimation algorithms are tested. Based on the real measurements, the performance is evaluated and compared with benchmark algorithms.

Human activities impact can be observed from the thermal model and the behavior pattern is an interesting problem remaining to consider. A more careful analysis of budget allocation is needed. The impact brought by HEM on the electricity price and real-time market warrants further studyis still an open problem. A number of simplifying assumptions made in this paper need to be justified for practical implementations. Nonetheless, many of the modifications required to circumvent the above simplification assumptions can be incorporated into the proposed optimization framework.

References

[1] D. Bargiotas and J. Birdwell, "Residential air conditioner dynamic model for direct load control ," *IEEE Trans. on Power Delivery*, vol. 3, pp. 2119 –2126, oct 1988.

[2] M. Y. Lamoudi, M. Alamir, and P. Béguery, "Distributed constrained model predictive control based on bundle method for building energy management," in *50th IEEE Conference on Decision and Control and European Control Conference*, Dec. 2011.

[3] R. Sonderegger, "Diagnostic tests determining the thermal response of a house," *Lawrence Berkeley Laboratory*, pp. 1 – 15, Feb. 1978.

[4] F. Schweppe, B. Daryanian, and R. Tabors, "Algorithms for a spot price responding residential load controller," *IEEE Trans. on Power System*, vol. 4, pp. 507–516, May 1989.

[5] D. L. Ha, S. Ploix, E. Zamai, and M. Jacomino, "Tabu search for the optimization of household energy consumption," in *2006 IEEE Int. Conf. Inf. Reuse Integr.*, pp. 86 – 92, 2006.

[6] M. A. A. Pedrasa, T. D. Spooner, and I. F. MacGill, "Coordinated Scheduling of Residential Distributed Energy Resources to Optimize Smart Home Energy Services," *IEEE Trans. on Smart Grid*, vol. 1, Sept. 2010.

[7] D. L. Ha, M. H. Le, and S. Ploix, "An approach for home load energy management problem in uncertain context," in *IEEE International Conference on Industrial Engineering and Engineering Management*, pp. 336 –339, Dec. 2008.

[8] A. Mohsenian-Rad and A. Leon-Garcia, "Optmal Residential Load Control With Price Prediction in Real-Time Electricity Pricing Environments," *IEEE Trans. on Smart Grid*, vol. 1, pp. 120–133, Sept. 2010.

[9] A. Brissette, A. Hoke, D. Maksimović, and A. Pratt, "A Microgrid Modeling and Simulation Platform for System Evaluation on a Range of Time Scales," in *IEEE Energy Conversion Congress and Exposition*, Sept. 2011.

[10] Y. Fu, N. Kottenstette, Y. Chen, C. Lu, X. D. Koutsoukos, and H. Wang, "Feedback Thermal Control for Real-time Systems," in *16th IEEE Real-Time and Embedded Technology and Applications Symposium*, pp. 111–120, Apr. 2010.

[11] M. Sznaier and M. J. Damborg, "Suboptimal control of linear systems with state and control inequality constraints," in *26th IEEE Conference on Decision and Control*, vol. 26, pp. 761 –762, Dec. 1987.

[12] N. L. Ricker, "Model predictive control with state estimation," *Industrial and Engineering Chemistry Research*, vol. 29, no. 3, pp. 374–382, 1990.

[13] G. Gattu and E. Zafiriou, "Nonlinear quadratic dynamic matrix control with state estimation," *Industrial and Engineering Chemistry Research*, vol. 31, no. 4, pp. 1096–1104, 1992.

[14] C. E. García, D. M. Prett, and M. Morari, "Model predictive control: Theory and practice-a survey," *International Federation of Automatic Control*, vol. 25, no. 3, pp. 335–348, 1989.

[15] A. Bemporad and M. Morari, "Robust model predictive control: A survey," *Lecture Notes in Control and Information Sciences*, vol. 245, pp. 207–226, 1999.

[16] L. Jia, Z. Yu, M. C. Murphy-Hoye, A. Pratt, E. G. Piccioli, and L. Tong, "Multi-Scale Stochastic Optimization for Home Energy Management," in *4th IEEE International Workshop on Computational Advances in Multi-Sensor Adaptive Processing*, pp. 113 – 116, Dec. 2011.

[17] Z. Yu, L. McLaughlin, L. Jia, M. C. Murphy-Hoye, A. Pratt, and L. Tong, "Modeling and Stochastic Control for Home Energy Management," in *2012 IEEE PES General Meeting*, Jul. 2012.

[18] L. McLaughlin, L. Jia, Z. Yu, and L. Tong, "Thermal Dynamic for Home Energy Management: A case study," Tech. Rep. ACSP-TR-10-11-01, Cornell University, Oct. 2011.

[19] A. Quiroga, Z. Yu, and L. Tong, "Home Energy Management system thermal dynamic model fitting," Tech. Rep. ACSP-TR-09-11-01, Cornell University, Sept. 2012.

[20] A. Hoke, A. Brissette, D. Maksimović, A. Pratt, and K. Smith, "Electric vehicle charge optimization including effects of lithium-ion battery degradation," in *IEEE Vehicle Power and Propultion Conference*, pp. 1–8, Sept. 2011.

[21] B. Li and A. G. Alleyne, "Optimal on-off control of an air conditioning and refrigeration system," in *American Control Conference*, pp. 5892 –5897, Jul. 2010.

[22] K. M. Tsui and S. C. Chan, "Demand Response Optimization for Smart Home Scheduling Under Real-Time Pricing," *IEEE Trans. on Smart Grid*, vol. 3, pp. 1812–1821, 2012.

[23] B. W. Olesen and K. C. Parsons, "Introduction to thermal comfort standards and to the proposed new version of EN ISO 7730," *Energy and Buildings*, vol. 34, pp. 537–548, 2002.